Research in Veterinary Science 172 (2024) 105244

Contents lists available at ScienceDirect

Research in Veterinary Science

journal homepage: www.elsevier.com/locate/rvsc

Isolation and characterization of mammary epithelial cells derived from Göttingen Minipigs: A comparative study *versus* hybrid pig cells from the IMI-ConcePTION Project

Chiara Bernardini [a,b], Salvatore Nesci [a], Debora La Mantia [a,*], Roberta Salaroli [a], Nina Nauwelaerts [c], Domenico Ventrella [a,b], Alberto Elmi [a], Fabiana Trombetti [a], Augusta Zannoni [a,b], Monica Forni [b,d]

[a] Department of Veterinary Medical Sciences, University of Bologna, Ozzano dell 'Emilia, 40064 Bologna, Italy
[b] Health Sciences and Technologies-Interdepartmental Center for Industrial Research (CIRI-SDV), Alma Mater Studiorum—University of Bologna, 40126 Bologna, Italy
[c] KU Leuven Drug Delivery and Disposition Lab, Department of Pharmaceutical and Pharmacological Sciences, KU Leuven University, Belgium
[d] Department of Medical and Surgical Sciences, University of Bologna, 40138 Bologna, Italy

ARTICLE INFO

Keywords:
Mammary epithelial cell
Large animal model
Miniature swine
Blood milk barrier
TEER measurements
Metabolic energetic profile

ABSTRACT

The value of pig as "large animal model" is a well-known tool for translational medicine, but it can also be beneficial in studying animal health in a one-health vision. The ConcePTION Project aims to provide new information about the risks associated with medication use during breastfeeding, as this information is not available for most commonly used drugs. In the IMI-Conception context, Göttingen Minipigs have been preferred to hybrid pigs for their genetic stability and microbiological control. For the first time, in the present research, three primary cell cultures of mammary epithelial cells were isolated and characterized from Göttingen Minipigs (mpMECs), including their ability to create the epithelial barrier. In addition, a comparative analysis between Göttingen Minipigs and commercial hybrid pig mammary epithelial cells (pMECs) was conducted. Epithelial markers: CKs, CK18, *E*-CAD, ZO-1 and OCL, were expressed in both mpMECs and pMECs. RT2 Profiler PCR Array Pig Drug Transporters showed a similar profile in mRNA drug transporters. No difference in energy production under basal metabolic condition was evidenced, while under stressed state, a different metabolic behaviour was shown between mpMECs *vs* pMECs. TEER measurement and sodium fluorescein transport, indicated that mpMECs were able to create an epithelial barrier, although, this turned out to be less compact than pMECs. By comparing mpMECs with mammary epithelial cells isolated from Hybrid pigs (pMECs), although both cell lines have morphological and phenotypic characteristics that make them both useful in barrier studies, some specific differences exist and must be considered in a translational perspective.

1. Introduction

For a useful translational biomedical research with a real clinical relevance, many different approaches must be persecuted, the use of the most appropriate animal model is the first step toward a relevant investigation (Gohar et al., 2018; Leenaars et al., 2019; Robinson et al., 2019). The last 20 years have seen a transition from an over-reliance on rodent models toward alternative animal models, including the pig species (Bin and Ning, 2016; Li and Fisher, 2023). Thanks to its high anatomical, physiological and metabolic similarity to human, swine has shown to be useful and reliable, by bridging the gap between simpler rodent models and humans (Karlsson et al., 2022; Kobayashi et al., 2018; La Mantia et al., 2022; Pabst, 2020; Sazzad et al., 2023; Sturek et al., 2020; Weber-Levine et al., 2022). In particular, miniature swine, known as minipig, has been utilized as translational research models for the study in the field of cardiovascular, dermal, digestive, urogenital, neurologic, ophthalmic, and musculoskeletal diseases (Forster et al., 2010; Singh et al., 2016; van der Laan et al., 2010). One of the most

* Corresponding author.
E-mail addresses: chiara.bernardini5@unibo.it (C. Bernardini), salvatore.nesci@unibo.it (S. Nesci), debora.lamantia2@unibo.it (D. La Mantia), roberta.salaroli@unibo.it (R. Salaroli), nina.nauwelaerts@kuleuven.be (N. Nauwelaerts), domenico.ventrella2@unibo.it (D. Ventrella), alberto.elmi2@unibo.it (A. Elmi), fabiana.trombetti@unibo.it (F. Trombetti), augusta.zannoni@unibo.it (A. Zannoni), monica.forni@unibo.it (M. Forni).

https://doi.org/10.1016/j.rvsc.2024.105244
Received 30 October 2023; Received in revised form 16 February 2024; Accepted 24 March 2024
Available online 27 March 2024

common breeds of minipig used in Europe, especially in pharmaceutical research, is the Göttingen Minipigs that is the result of a crossing of three different breeds: the Minnesota Minipig, the Vietnamese Potbelly and the German Landrace. They are specifically selected for small size, genetic stability, health status, all these aspects make them a very helpful model for biomedical research (Bollen and Ellegaard, 1997; Flisikowska et al., 2022; Simianer and Köhn, 2010). The animal model standardization, by assuring high level of genetic and microbiological controls, is a prerequisite to practice Reduction and, in mean time, to achieve reproducible research results (Festing, 2004). Within the framework of the IMI funded ConcePTION Project (ConcePTION, n.d.), with the aim of filling the huge gap in scientific information concerning the safe use of medicines during pregnancy and breastfeeding, the pig has been selected as the most appropriate animal model (Ventrella et al., 2021), and in particular Göttingen Minipigs are selected as the best breed. In full compliance of both international legislations and the 3Rs principles, to limit the use of animals for experimentation, ConcePTION Project also explored the parallelisms of results between *in vivo* and *in vitro* studies, aiming to achieve at least partial Replacement solutions. In this context, we recently published a new efficient method to isolate, expand and culture Mammary Epithelial Cells from hybrid pig tissues collected at the slaughterhouse, for studying the mammary epithelial barrier *in vitro* (Bernardini et al., 2021b). Indeed, *in vitro* cell cultures could represent a powerful tool for pre-screening studies and, to better represent the *in vivo* conditions, primary cell cultures are preferred to immortalized cell lines for their superior physiological relevance and reduction of misidentification or contaminations problems (Rojas et al., 2008). Due to the increasing use of Göttingen Minipigs as an *in vivo* animal model, some doubts arise as to whether *in vitro* results obtained in already available hybrid pig cell lines can be compared with the *in vivo* results obtained in this specific breed (Müller et al., 2013). Differences have also been reported at the metabolic level in relation to the breed of pig used, and these are particularly relevant when attempting to predict human pharmacokinetic parameter values on the basis of data obtained in pigs. In addition, *in vitro* and *in vivo* correlation (IVIVC) in the pig animal model may increase the reliability of results obtained by *in vitro* methods utilizing human cells (Tang and Mayersohn, 2018).

In the present research we have applied our previously established isolation method (Bernardini et al., 2021b), on the Gottingen Minipigs mammary gland tissues, thus obtaining primary cell lines that we have fully characterized and expanded. Then, to offer a complete set of information on the possible model for studying the mammary epithelial barrier, we conducted a comparative analysis between Göttingen Minipigs and commercial hybrid pig mammary epithelial cells (mpMECs and pMECs respectively), including the cellular bioenergetic metabolism, the ability to create mammary epithelial barrier and the expression of many drug transporters genes.

2. Material and methods

2.1. Chemicals and reagents

Dulbecco Phosphate Buffered Saline (DPBS) with calcium and magnesium, Fetal Bovine Serum (FBS), trypsin-EDTA, Antibiotic-Antimycotic 100× (15240062), gentamicin, recombinant human epidermal growth factor (hEGF), Dulbecco's Modified Eagle Medium: Nutrient Mixture F-12 (DMEM/F12), Hanks Balanced Salt Solution (HBSS) with calcium and magnesium, RNaseA/T1 were purchased from Thermo Fisher Scientific (Waltham, MA, USA). Propidium iodide (PI) and Multi Tissue Dissociation Kit1 were purchased from Miltenyi Biotec (Bergisch Gladbach, Germany). TRI Reagent was purchased from Molecular Research Center In, OH, USA and NucleoSpin RNA II kit from Macherey-Nagel GmbH & Co. KG, Düren, Germany. RT2 First Stand Kit, RT2 SYBR Green qPCR Mastermix and RT2 Profiler™ PCR Array Pig Drug Transporters (Cat. No. PASS-070ZD) were purchased from Qiagen Hilden, Germany. Dimethyl sulfoxide (DMSO), Diaminobenzidine, FluoroshieldTM with DAPI histology mounting medium, glucose and 2-[4-(2-hydroxyethyl) piperazin-1-yl] ethanesulfonic acid (HEPES) were purchased from Sigma-Aldrich (St. Louis, MO, USA). Betadine 10% cutaneous solution was purchased from Meda Pharma Spa (Milan, Italy). Sodium fluorescein was purchased from Siegfield Zofingen (Switzerland) and used at 1 mg/mL. The culture medium used for cell isolation, named Isolation Medium (Im), was the Mammary Epithelial Cell Medium supplemented with 0.004 mL/mL Bovine Pituitary Extract (BPE), 10 ng/mL hEGF, 5 μg/mL insulin, 0.5 μg/mL hydrocortisone purchased from Promo Cell (Heidelberg, Germany), 1% an-ti-anti and 50 μg/mL gentamicin. All plastic supports for primary cell culture were purchased from Corning-Beckton-Dickinson (Franklin Lakes, NJ, USA). The medium used for cell expansion named Expansion Medium (Em) was composed of DMEM/F12 with 10% FBS, 5 μg/mL insulin and 0.5 μg/mL hydrocortisone (both provided by Promo Cell), 5 ng/mL hEGF (provided by Thermo Fisher) and 1% anti-anti. The medium used for metabolic energetic profile, and RT2 Profiler PCR array for Pig Drug Transporter was: Mammary Epithelial Cell Growth Medium (MECGM), composed by with 0.004 mL/mL Bovine Pituitary Extract (BPE), 10 ng/mL hEGF, 5 μg/mL insulin, 0.5 μg/mL hydrocortisone purchased from Promo Cell (Heidelberg, Germany), 1% anti-anti. For barrier study cell were grown in Em then HBSS with addition of 10 mM HEPES and 25 mM glucose (Transport buffer Tb): was used for trans-epithelial electrical resistance (TEER) measurement, and sodium fluorescein (SF) transport analysis. The antibodies used for the immunofluorescence (IF) and flow cytometry analysis (FC) are listed in the Table 1.

2.2. Animal description

All methods were performed in accordance with the relevant guidelines and regulations. Tissue samples were collected from animals enrolled in an experimental lactation study, within the ConcePTION project framework. Approved by the Italian Ministry of Health as dictated by D.Lgs 26/2014 (approval n° 32/2021-PR; all procedures were performed in compliance with ARRIVE guidelines). At the end of the experimental trial, sows, acquired by Ellegaard Göttingen Minipigs A/S (Dalmose, DK), were group housed with a light: dark cycle of 12:12 hand fed with a standard commercial diet (Micropigs 9AB20; Mucedola srl, Settimo Milanese MI, IT). Pens were equipped with both chewable and wooden environmental enrichment. In order to give time to the mammary glands to go back to a non-milk producing status, six months from the last weaning day was waited. On the day of sacrifice, animals were sedated intramuscularly (IM) with 5 mg/kg of tiletamine/zolazepam (Zoletil, Virbac, Carros, FR) and euthanized upon barbiturate overdose (Sodium thiopental 60 mg/kg; Pentothal sodium, MSD Animal Health srl, Madison, NJ, USA).

Table 1
List of antibodies used for immunofluorescence (IF) and flow cytometry (FC) analysis.

Antibody	P. Number	Host Specie	Supplier	Application
Anti CK	GA053	Mouse	Agilent Dako	IF: 1:150
Anti ZO-1	61–7300	Rabbit	Thermo Fisher	IF: 1:100
Anti OCL	H-279	Rabbit	Santa Cruz Biotechnology	IF: 1:50
Anti-Rabbit IgG-Alexa Fluor 488	A11034	Goat	Thermo Fisher	IF: 5 μg/mL
Anti-Mouse IgG-Alexa Fluor 594	A11032	Goat	Thermo Fisher	IF: 5 μg/mL
Brilliant Violet 421™ anti-*E*-cadherin	147,319	Rat	BioLegend	FC: 17 μL/10^6
FITC anti-cytokeratin 18	ab52459	Mouse	Abcam	FC: 10 μL/10^6

2.3. Cell isolation

Göttingen Minipigs mammary gland (MG) tissues were collected from sows (n = 3) in order to obtain three primary mammary epithelial cell lines (MG9, MG11 and MG12 mpMECs respectively). The mammary line tissue was immediately transferred to the laboratory in a temperature-controlled container (+4 °C); before cell isolation the tissue was disinfected with Betadine (10% cutaneous solution) and ethanol 70%. Portions of mammary glands were isolated and collected for hystological examination and cell were isolated by combining enzymatic and mechanical dissociation using the Miltenyi GentleMACS Octo Dissociator, as previously described by (Bernardini et al., 2021b). At confluence 70%, the cells were detached with trypsin-EDTA 1× solution, counted and seeded into a T-25 primary culture flask until 70–75% confluence was reached (first passage P1).

2.4. Histological examination

Samples of mammary gland of 1 cm^3 were embedded in OCT and frozen in isopentane cooled in liquid nitrogen. Seven micrometers-thick sections were cut with a Leica CM1950 cryostat (Leica, Wetzlar, Germany), then left to adhere to a microscope slide and stained with hematoxylin and eosin (H&E) according to as previously described (Bernardini et al., 2021b). Images were obtained using a Nikon digital camera (DS-Qi2 Monochrome Digital Microscope Camera), installed on a Nikon epifluorescence microscope Eclipse E600 and analysed with digital image software NIS-Elements BR Ver5.30.00 (Nikon, Tokyo, Japan).

2.5. Cell characterization: flow-cytometry and immunofluorescence analysis

To confirm the epithelial origin of isolated cells: cytokeratins (CKs), cytokeratin 18 (ck18) and epithelial cadherin (*E*-Cad) were evaluated. To study ck18 and E-Cad, flow Cytometry analysis was performed as previously described (Bernardini et al., 2021b). Briefly, cells were fixed in paraformaldehyde and permeabilized in methanol then cells were incubated with anti-E-cadherin or anti-cytokeratin 18 antibodies (Table 1). Negative controls were obtained omitting primary antibodies. Cells were analysed with the MacsQuant Analyzer10 (Miltenyi Biotec, Bergisch Gladbach, Germany) and the Flowlogic™ software (Inivai Technologies, Mentone Victoria, Australia). To start, cellular events were discriminated from debris using forward (FSC-A) *vs.* side scatter (SSC-A). Doublets' exclusion was obtained by plotting FSC-area *vs* height (FSC-A/FSC-H). The fluorescent staining intensity was determined comparing the median intensity fluorescence (MFI) of the negative control and the MFI of single stained cells. To study CKs, ZO-1 and OCL the cells were seeded on an 8-well slide chamber (BD Falcon Bedford, Franklin Lakes, NJ, USA) at a concentration of 5×10^4 cells/well. After 24 h, the cells were washed in DPBS and fixed in 4% paraformaldehyde for 15 min at RT. Subsequently, fixed cells were permeabilized with 0.5%Triton-X 100 in DPBS for 15 min at RT and then blocked with 0.5% Triton-X 100, 10% FBS in DPBS (blocking solution) for 1 h at room temperature. Then, cells were incubated ON at 4 °C in a humid atmosphere with the primary antibodies and images were obtained using a Nikon digital camera (DS-Qi2 Monochrome Digital Microscope Camera), installed on a Nikon epifluorescence microscope Eclipse E600 and analysed with digital image software NIS-Elements BR Ver5.30.00 (Nikon, Tokyo, Japan).

2.6. Cell expansion

mpMECs were expanded from P1 to P10 in the Expansion medium in T25 or T75 primary culture flasks and doubling time was calculated as previously described (Zaniboni et al., 2014). Aliquots of 0.5×10^6 or 1×10^6 were cryopreserved in 1 mL of freezing medium (90% FBS and 10% DMSO). Aliquots of cell culture medium were periodically collected and analysed by the EZ-PCR Mycoplasma Detection kit to ascertain the possible mycoplasma contamination.

2.7. Cell cycle evaluation

At the end of the expansion procedure, aliquots of 1×10^6 cells were washed twice in 5 mL of DPBS without calcium and magnesium and fixed overnight in 70% ice-cold ethanol (1 mL) added drop-by-drop with continuous vortexing. Then, the cells were washed twice with 10 mL of DPBS without calcium and magnesium. The cell suspensions were filtered through a 70 μm MACS Smart Strainers (Miltenyi Biotec) then the cellular pellet was incubated with 1 mL of staining solution containing 50 μg/mL of PI and 100 μg/mL RNaseA/T1 in DPBS without calcium and magnesium for 45 min in the dark at room temperature with gentle rocking. Cell distribution in cell cycle phases was analysed by MACSQuant®Analyzer10 and Flowlogic™software (Inivai Technologies, Australia) as previously described (Levi et al., 2021). Experiment was repeated three times. Dean Jett Fox model was used to determinate the percentage of cells across the cell cycle. DNA index (DI) was calculated as the ratio between the mean G1 fluorescence level in MG9, MG11 and MG12 cells and that of the diploid granulosa cells from porcine ovaries obtained from a local slaughterhouse. A DI of 1.0 represents a normal diploid DNA content.

2.8. Trans-epithelial electrical resistance (TEER) measurement and sodium fluorescein (SF) transport

The ability of mpMECs to form an intact monolayer was assessed through the measurements of the TEER and SF transport as previously described (Bernardini et al., 2021b). For the characterization of the monolayer integrity, cells were seeded at different density (0.1, 0.15, 0.2 and 0.3×10^6 cells) and cultured on transparent polyester permeable supports of pore size 0.4 μm; membrane area 0.3 cm^2. Resistance measurements were taken in Tb at 37 °C using an Epithelial Volt/Ohm Meter (Millicell ERS-2 Voltohmmeter® (Millipore, Billerica, MA) and TEER was calculated using the eq. 1 (Eq. 1), where Rcells was the mean resistance measured in cell inserts, Rblank was the mean resistance measured in the blank inserts and Marea was the area of the membrane. Permeability flux assay with SF tracer was then assessed following the protocol previously described (Bernardini et al., 2021b). Briefly, 2.66 mM SF in Tb was added to the apical compartment (0.5 mL) and only Tb (1.2 mL) added to the basal compartment. The concentration of SF in the samples, derived from the basolateral compartment (after 1 h incubation), was measured *via* fluorescence intensity at excitation/emission λ = 485/535 nm using Appliskan® microplate reader (5,230,000 Appliskan 120-240 V, Thermo Fisher Scientific). The percentage of sodium fluorescein transport was calculated using the Eq. 2 where Csample was the concentration of SF in the sample, C_0 was the SF donor concentration, V_b was the volume of the basolateral compartment and V_a was the volume of the apical compartment.

$$TEER\ \left(\Omega^{*}cm^2\right) = \left[R_{cells}(\Omega) - R_{blank}\ (\Omega)\ \right] \times M_{area}\ \left(cm^2\right) \quad (1)$$

$$Transport\ (\%) = \left(\frac{Csample}{C0}\right) \times \left(\frac{Vb}{Va}\right) \times 100 \quad (2)$$

2.9. Comparative study: Göttingen Minipigs vs hybrid pig cells

To analyse the potential differences between mammary epithelial cells isolated from Göttingen Minipigs with cells isolated from hybrid commercial pig, a comparative study was conducted. To avoid single animal differences, a pool of the three different mpMECs primary cell lines and a pool of three primary cell lines previously isolated from hybrid pig (Bernardini et al., 2021b) were used. To generate the cellular pools, cells were thawed and cutured till 70% of confluence; then were

detached, counted and mixed: one pool of minipig cells named mpMEC pool and one pool of hybrid pig cells named pMEC pool were generated respectively. Cellular pools were expanded for some passages, the epithelial morphology was carefully monitored, and the doubling time was calculated. The two different cellular pools were used for comparative study of metabolic energetic profile, barrier study and drug transporter gene expression analysis in three independent experiments.

2.10. MEC metabolic energetic profile

MpMECs pool and pMECs pool were cultured in MECGM, then measurement of oxygen consumption rate (OCR), cellular respiration rate (pmol/min) and extracellular acidification rate (ECAR), glycolysis rate (mpH /min), was performed using the Seahorse XFp Analyzer (Agilent, USA). mpMEC and pMECs (2×10^4/well) were grown in XFp cell culture miniplates (Agilent, USA) for 24 h. On the day of the experiment, cells were switched to a freshly made Seahorse XF DMEM medium of pH 7.4 supplemented with 10 mM glucose, 1 mM sodium pyruvate, and 2 mM L-glutamine. The OCR and ECAR were measured with the ATP Rate Assay, Cell Mito Stress Test, Cell Energy Phenotype Test and Glycolysis Stress Test programs after the plates were incubated for 45 min at 37 °C in air. In addition, the injection ports of the XFp sensor cartridges were hydrated overnight with XF calibrant at 37 °C; they were subsequently loaded with 10× the concentration of inhibitors, as indicated by the instructions for the Seahorse XFp ATP Rate Assay, Cell Mito Stress Test, Cell Energy Phenotype Test and Glycolysis Stress Test. Final concentrations of 1.5 μM oligomycin (port A) and 0.5 μM rotenone (Rot) plus 0.5 μM antimycin A (AA) (port B) were used for the ATP Rate Assay. Instead, for the Cell Mito Stress Test, the final concentrations were 1.5 μM oligomycin (olig) (port A), 1.0 μM carbonyl-cyanide-4-(trifluoromethoxy) phenylhydrazone (FCCP) (port B), and 0.5 μM rotenone plus antimycin A (port C) (Bernardini et al., 2021a). For the Cell Energy Phenotype Test the final concentrations were 1.5 μM oligomycin plus 1.0 μM FCCP (port A). Finally, for the Glycolysis Stress Test the concentrations used were 10 mM glucose (port A), 1 μM oligomycin (port B), and 50 mM 2-deoxyglucose (2DG) (port C). The energy parameters provided by the ATP Rate Assay, Cell Mito Stress Test and Glycolysis Stress Test have already been reported by Algieri et al. (Algieri et al., 2022) and for Cell Energy Phenotype Test by Bernardini et al. (Bernardini et al., 2021a). All the analysis was run at 37 °C. All data were analysed by WAVE software version 2.6.1. OCR and ECAR values were normalized to the total number of cells per each well by Burker counting chamber. All parameter values were calculated per well according to the manufacturer's instructions. ATP Rate Assay, Mito Stress Test, Cell Energy Phenotype Test and Glycolysis Stress Test were carried out in three independent experiments.

2.11. MEC barrier study

mpMEC pool and pMEC pool were cultured on transparent polyester permeable supports of pore size 0.4 μm and a membrane area of 0.3 cm^2. The cellular monolayers were assessed by checking the expression of ZO-1 and OCL. Cells were washed in DPBS and fixed in 4% paraformaldehyde for 15 min at RT. After fixation the cells were permeabilized with 0.5%Triton-X 100 in DPBS for 15 min at RT and then blocked with 0.5%Triton-X 100, 10% FBS in DPBS for 1 h at room temperature. Then, the cells were incubated overnight at 4 °C with the primary antibodies (see Table 1) diluted in DPBS. After being rinsed in PBS (3 times 10 min each), the cells were incubated with fluorochrome-labeled secondary antisera diluted in DPBS 1 h at RT (Table 1). After 3 washes (10 min each) in PBS, the membrane was detached from the transwell and placed on slide. Mounting medium with DAPI to counterstain the nuclei was added on slide and on top of the membrane. Images were obtained using Nikon digital camera (DS-Qi2 Monochrome Digital Microscope Camera) installed on a Nikon epifluorescence microscope Eclipse E600 and analysed with digital image software NIS-Elements BR Ver5.30.00 (Nikon, Tokyo, Japan). The intact monolayer was assessed through the measurements of the Trans-epithelial electrical resistance measurement and sodium fluorescein (SF) transport as described above.

2.12. MEC drug transporter study

MpMEC pool and pMEC pool were cultured in MECGM till confluence then RNA extraction was performed on the pre-mixed pool of mpMECs (1×10^6 cells) using TRI Reagent and the NucleoSpin RNA II kit, as previously described (Tubon et al., 2019). After spectrophotometric quantification (DeNovix DS-11, DeNovix Inc.,Wilmington, NC, USA) total RNA (500 ng) was reverse-transcribed to cDNA using the RT2 First Stand Kit and RT2 Profiler™ PCR Array Pig Drug Transporters were performed as previously described (Bernardini et al., 2021b; Bernardini and Nauwelaerts, 2021). Gene expression of 84 transepithelial transporter genes was analysed using the ΔCt method (mean Ct Reference Gene (R.G.) —Ct Interest Gene (I.G.)), according to the RT2 Profiler PCR Array Handbook.

2.13. Statistical analysis

Doubling time, cell cycle, TEER and SF Transport data were analysed by one-way analysis of variance (ANOVA) followed by the *post hoc* Tukey comparison test ($p < 0.05$) (GraphPad Prism 5 software). Flow Cytometry and array data were analysed with Student's *t*-test comparing MFI of the negative control and the MFI of single stained cells ($p < 0.05$) in each cell lines.

All bioenergetic profile data were analysed by WAVE software version 2.6.1; OCR and ECAR values were normalized to the total number of cells per each well. All parameter values were calculated per well according to the manufacturer's instructions.

3. Results

3.1. Cells isolated from Göttingen Minipigs mammary glands showed epithelial cell morphology and expression of epithelial cell markers

Samples obtained from all the three minipigs showed resting mammary gland with variable mixture and proportion of adipose tissue and dense collagen stroma, embedding mammary interlobular and intralobular ducts. True functional alveoli with lumen containing secreted material were absent in all the three mammary glands. (Fig. 1a'-a'''). Few days after isolation cluster cells were attached in all the three mammary gland samples (Fig. 1b'-b'''). Cell cluster grew (Fig. 1c'-c''') and reached confluence about three weeks after isolation, showing a typical epithelial morphology with cobblestone-like shape (Fig. 1d'-d'''). Overall, primary cell cultures of mammary epithelial cells were obtained from all the three Göttingen Minipigs with a medium value of $2.2 \pm 1.3 \times 10^5$ cells/g of tissue. Immunofluorescence analysis showed that the cells expressed diffusely cytokeratins (Fig. 2 a'-a'''). Quantitative flow cytometry analysis revealed that all the three minipig cell cultures expressed the mammary epithelial specific intermediate filament protein cytokeratin-18 (CK18, Fig. 2 b'-b''') and the cell adhesion protein epithelial-cadherin (*E*-Cad, Fig. 2c'-c'''). Both CK18 and E-Cad positive peaks had a bright fluorescence intensity indicating positivity of the whole cellular populations (Fig. 2 b'-b''' and c'-c'''). In MG12, the contour of CK18 positive peak showed a shoulder suggesting the presence of a cellular subpopulation with a particularly high positivity (Fig. 2 b''').

The three primary cell cultures were successfully expanded till passage 10, MG9 resulted slower at passage two than the other cultures (Fig. 3a). The cumulative mean doubling time confirmed MG12 the fastest, while MG9 the slowest (Fig. 3b). Regarding cell cycle, MG9, MG11 and MG12 showed the three distinct phases that could be recognized in a proliferating cell population: G0/G1, S and G2/M (Fig. 3c). The DNA index was normal for all three cell populations, with

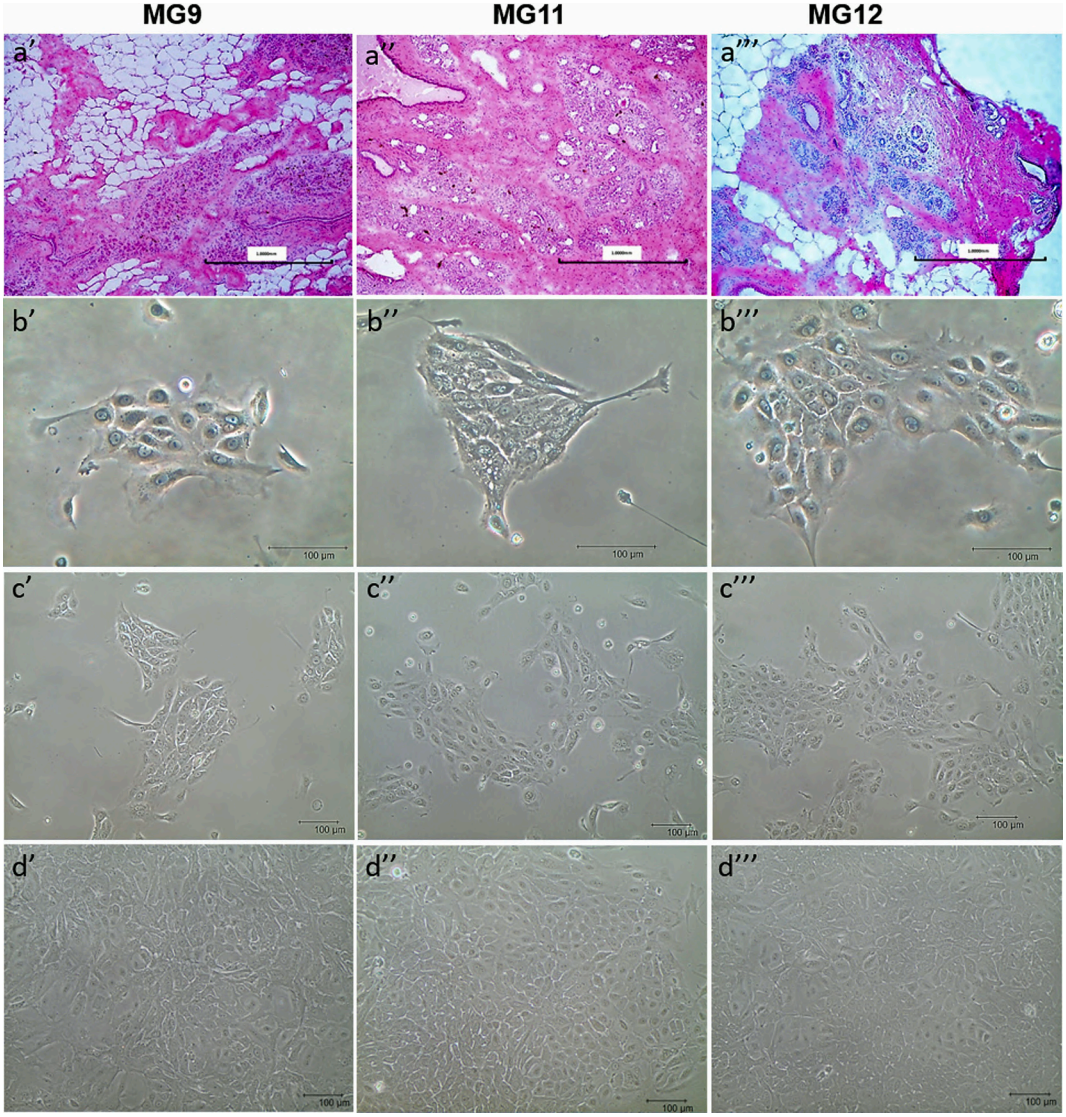

Fig. 1. Cells isolation from minipig mammary glands Representative Hematoxylin and Eosin (H&E) pictures of abdominal MG9, MG11 and MG12 mammary gland showing glandular parenchyma with interlobular and intralobular ducts (a'-a'''). Representative images of cell cluster after few days post isolation (b'-b''' and c'-c'''). Typical epithelial cell morphology (c'-c'''), cells reached confluence after about three weeks (d'-d'''). Scale bar = 1 mm(a'-a'''), scale bar = 100um (b'-b'''; c'-c'''; d'-d'').

a mean value of 0.98 ± 0.01. All the cultures were detected as negative for mycoplasma contamination during expansion (data not shown).

3.2. Cells isolated from Göttingen Minipigs mammary glands showed the ability to form the epithelial barrier

The formation of the monolayer integrity was evaluated *via* TEER measurement and SF percentage of paracellular fluorescent tracer transport (Fig. 4). The three primary cell cultures formed a compact monolayer following different kinetics at the cell seeding density tested. The TEER measurement and the SF profile concorded, in fact the paracellular flux of the tracer SF across the epithelial monolayer was always lower than 0.3% when TEER was high. Similar TEER profile and SF values were detected only when cells were seeded at density of 0.15×10^6 cells, in particular, at the day 3 and 4 of culture, all the three primary lines resulted in an achieving higher TEER and lower SF values (Fig. 4 a-h). By comparing the maximum values of TEER reached at the different seeding density tested (Fig. 4g), a significative difference resulted in MG9 with respect to MG11, MG12; the kinetic profile is very different too, MG9 compact monolayer is stable for more days when seeded at the higher cell density.

3.3. Comparative study between mammary epithelial cells isolated from Göttingen Minipigs and hybrid pigs

No differences in morphology or epithelial marker expression were detected between mpMECs and pMECs pool: both primary cell lines exhibited a cobblestone-like morphology and well expressed the specific epithelial markers like as cytokeratins (CKs), cytokeratin 18 (CK18), epithelial cadherin (*E*-Cad), Zonula Occludens-1 (ZO-1) and Occludin (OCL)(Bernardini et al., 2021b). A different rate of growth existed: mpMECs growth faster than pMECs, in fact the average value of doubling time was 30,19 ± 3,80 h for mpMECs while 46,20 ± 2,71 for pMECs.

3.4. Bioenergetic profile: mpMECs and pMECs are similar in energy production under basal cell culture but responded differently at stress conditions

The ATP rate production was obtained from OCR and ECAR values

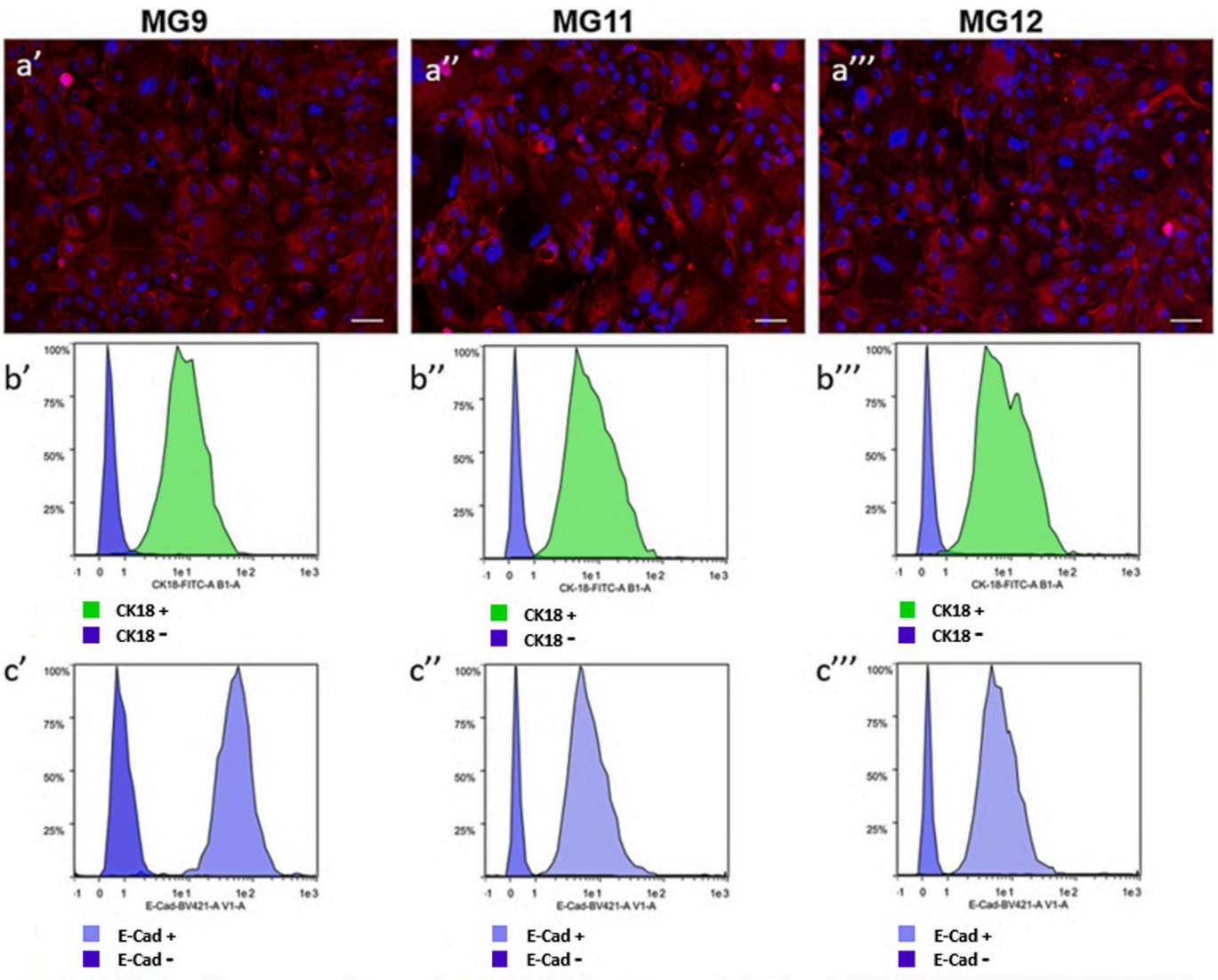

Fig. 2. Expression of epithelial cell markers in isolated cells Immunofluorescence analysis of Citokeratins in MG9, MG11 and MG12 respectively (a'-a'''). Nuclei are stained with DAPI (blue), scale bar = 100 μm. Flow cytometric analysis of epithelial markers CK18 (b'-b''') and E-Cad (c'-c'''). Each graph shows the percentage of cells expressing E-Cad or CK18 (purple or green Area Under the Curve—AUC) and the relative negative control (blue AUC, cells not incubated with any antibodies). (For interpretation of the references to colour in this figure legend, the reader is referred to the web version of this article.)

under basal conditions. The depicted kinetic results of OCR and ECAR measurement allowed the calculation of the mitoATP and glycoATP production rate (Fig. 5a). However, mpMECs and pMECs showed no difference in energy production as well as highlighted by the energy map profile (Fig. 5b). Moreover, the mitoATP production rate and glycoATP production rate (ATP rate index) was >1 (Fig. 5b), which means a less glycolytic and more oxidative phenotype.

The cell energy production detected by OCR and ECAR in mpMECs and pMECs was shown as a metabolic phenogram under normal (baseline) and stressed conditions in the presence of oligomycin plus FCCP mixture. The treatment with mitochondrial stressors provided the phenogram that illustrated the relative baseline and stressed phenotype, and the response of the metabolic potential (expressed as % baseline) of cells. According to the method adopted, the investigated cell lines revealed an energetic profile with a rise in energetic metabolism *via* cellular respiration and glycolysis defined as the % increase in the stressed phenotype over the OCR and ECAR baseline phenotype (Fig. 5c). The metabolic potential of stressed OCR or stressed ECAR, which indicates the cell's ability to meet energy demand through mitochondrial respiration and glycolysis to satisfy the cell energy demand, doubled in both mpMECs and pMECs although was significantly higher in pMECs than mpMECs (Fig. 5d).

To evaluate any metabolic differences, analyses of mitochondrial bioenergetics and the glycolysis pathway have been performed. The cell respiration profile of mpMECs and pMECs is shown in Figure 5e. The key parameters of mitochondrial activities, known as basal respiration, were detected as the baseline OCR before the addition of oligomycin; the minimal respiration, measured as the OCR in the presence of oligomycin that corresponds to the proton leak; the maximal respiration, evaluated as the OCR after the addition of FCCP; spare respiratory capacity provided from the difference between the maximal and basal respiration; and ATP turnover, as the oligomycin-sensitive OCR has been calculated (Fig. 5f). We revealed statistically significant differences in basal respiration, maximal respiration, and ATP turnover between mpMECs and pMECs.

The glycolysis cells detected as ECAR presented different profiles for mpMEC and pMEC (Fig. 5g). Glycolytic Capacity and Glycolytic Reserve, the latter defined as the difference between Glycolytic Capacity and Glycolysis, are two crucial glycolytic flow parameters that are higher in the mpMEC than in the pMEC (Fig. 5h).

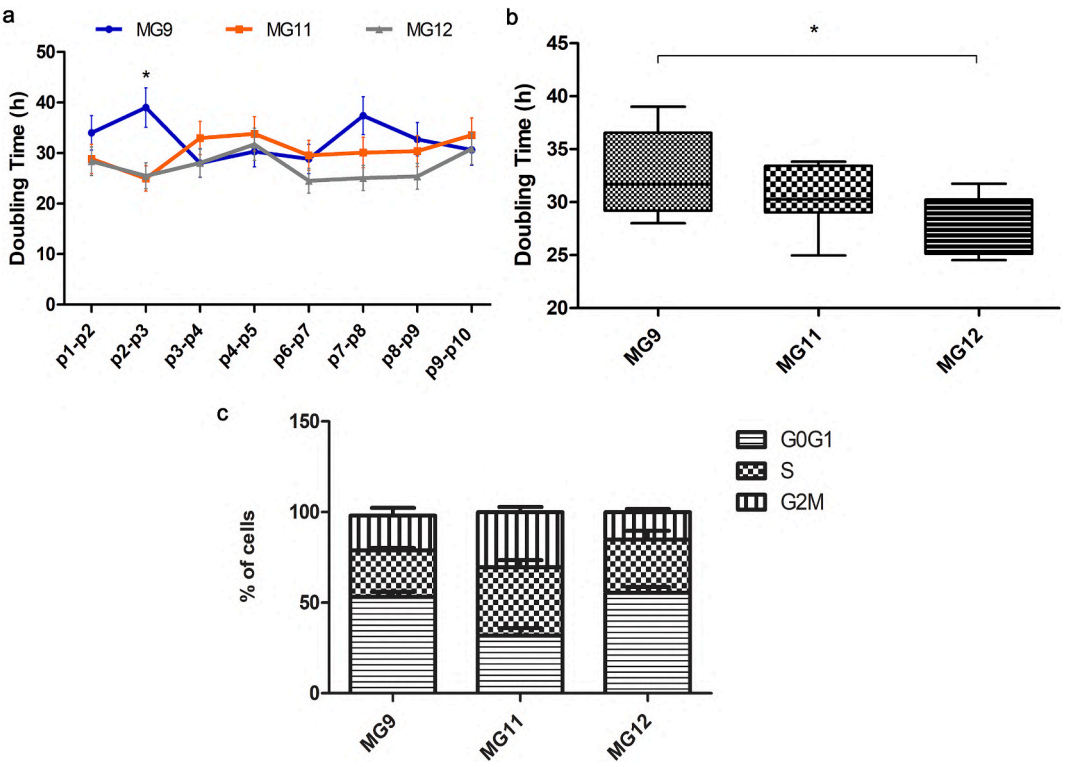

Fig. 3. Primary Mammary epithelial cells expansion a) mpMEC growth curve (passage 1 to 10) for each cell line is represented, doubling time is expressed in hours, b) Doubling time mpMEC boxplots represented as of each cell line where the two segment that delimit the rectangle represented the 25th and 75th percentiles, the central segment was the median and the bars the minimum and maximum values respectively. Data were analysed with a one-way analysis of variance (ANOVA) followed by the *post hoc* Tukey's multiple comparison test (*$p < 0.05$) (n = 3). graph data represent the mean ± SEM of the duplication time from P1 to P10 for each cell line c) Distribution across cell cycle phases of the three primary cellular line at the end of expansion phae, sacked bar chart shows cellular distribution across cell cycle phases (G0/G1, S and G2/M).;

3.5. Cell barrier study: mpMECs formed a less tight compact barrier than pMECs and showed a similar drug transporter expression profile

Both mpMECs and pMECs created a compact monolayer on transwell expressing tight junctions ZO-1 and OCL (Fig. 6a). For mpMECs, a plateau in TEER values (±173 Ωcm2) was reached after three days and remained stable for 24 h, followed by a quick drop (Fig. 6b). Accordingly, SF transport, reached optimum values, <0,3% at day three and remained stable for 24 h (Fig. 6b). pMECs showed a different pattern in both TEER and SF transport, higher values of TEER, with a maximum of +/− 720,5 Ωcm2 reached at the day 2 that remain so up to day 4. Accordingly, fluorescein sodium transport was minimum (0,08%) from day 2 to day 4 (Fig. 6b). The TEER value maximum and SF transport minimum value indicated that mpMECs formed a less tight compact barrier than pMECs (Fig. 6c).

No difference between mpMECs and pMECs drug transporter gene expression levels was observed (Fig. 7). Among the 84 genes, 66 genes were detectable, 18 genes were not detectable or higher than 35 threshold cycle, so considered as negative according to the handbook, in both cell lines (ABCA13, ABCA9, ABCB11, ABCB4, ABCC12, ABCD2, ABCG2, ABCG8, AQP9, SLCO1B3, SLC18A1, SLC22A1, SLC2A2, SLC47A2, SLC7A2, SLC7A9, SLC22A3 and SLC22A8).

4. Discussion

Recent studies have shown that every year, the paucity of information on the safety of using drugs during pregnancy and breastfeeding, causes millions of women to give up breastfeeding, because of the pharmacological treatments they have to undergo (Adam et al., 2011; Nörby et al., 2021; van der Graaf et al., 2019; Ventrella et al., 2021).

Within the framework of the Europe Horizon programme, in particular the European Partnership for "Innovative Medicine Initiatives", many studies on the passage of medicines into milk have been encouraged and supported through the funding of the ConcePTION project (ConcePTION, n.d.) that chosen a multidisciplinary and transversal approach that involves the development of *in vivo*, *in vitro* and *in silico* models. The pig species has been proposed as an elective animal model preferring the Göttingen minipigs breed *vs* commercial hybrid pig for a more genetic standardization and a more microbiological control of the animal model (Ashkenazi and Ventrella, 2020). In order to improve studies involving *in vitro* and *in vivo* correlation (IVIVC), the ConcePTION Consortium chose to work with primary cell cultures than immortalized cell lines to better preserve the *in vivo* epithelial phenotype, in a translational perspective (Bernardini et al., 2023; Bernardini and Nauwelaerts, 2021).

Since previous studies (Dahanayaka et al., 2015) indicated that cellular viability was very low in lactating sows, we isolated cells from three different multiparous Göttingen sows with resting mammary glands, six months from the last weaning. Histological investigation confirmed that no secretive component was present, even if many branching ducts were detectable in all the samples.

We successfully isolated primary cells from all the three animal glands, confirming the reliability and optimization of our previously defined isolation protocol (Bernardini et al., 2021b); the morphology and immunophenotypization analysis confirmed the epithelial phenotype. Moreover, all the three primary cell cultures resulted positive for epithelial-Cadherin. Expansion phase was successfully conducted, and no cell cycle abnormalities were observed.

A main characteristic of mammary epithelial cells is the ability to create a biological barrier, the development of *in vitro* models mimicking the mammary epithelial barrier function is a useful tool to study the potential xenobiotics passage in milk. Recent review underlined that

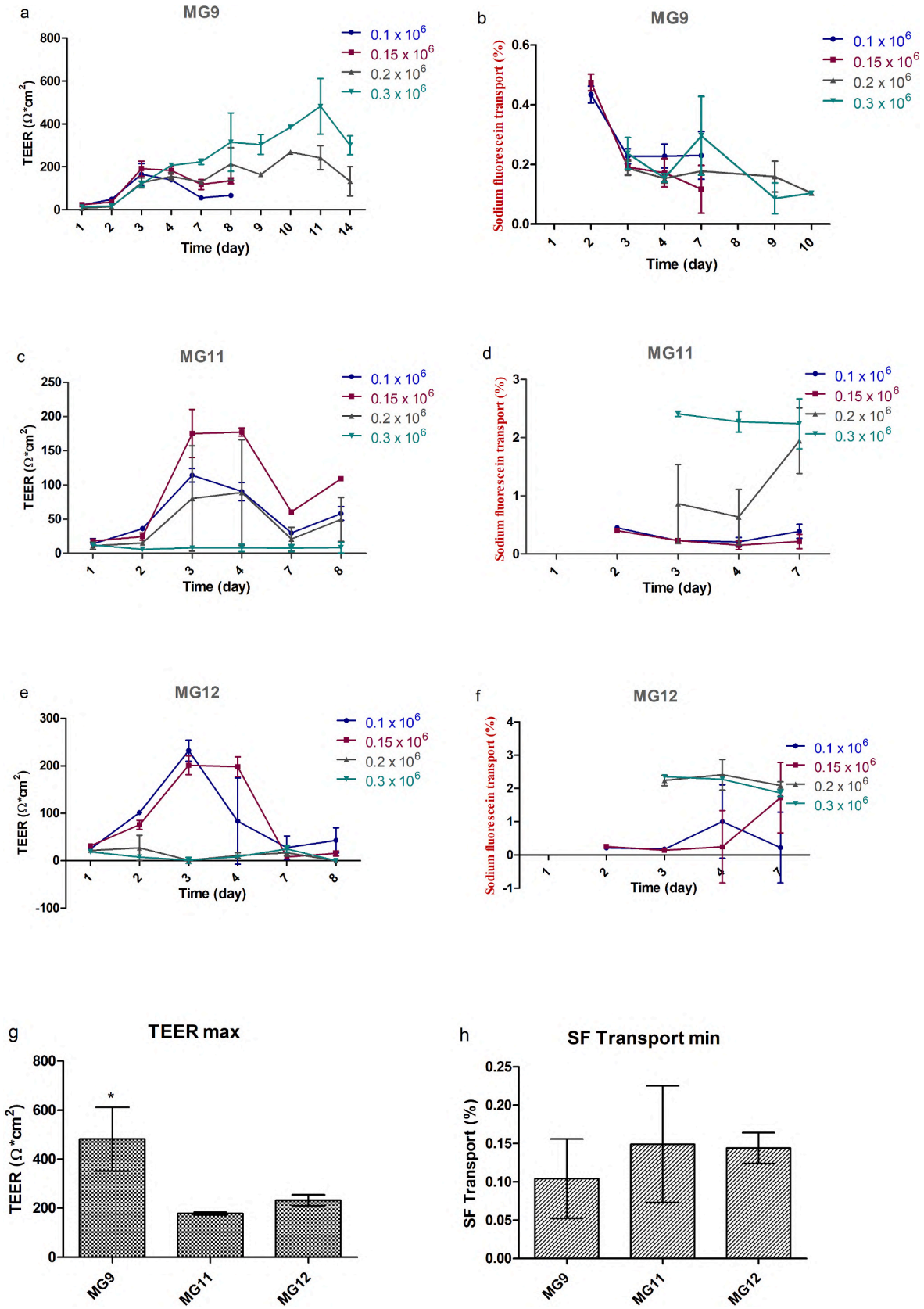

Fig. 4. mpMEC barrier formation. (a – f) TEER (Ω*cm^2), graphs on the left and, SF transport (%), graphs on the right, profiles for each primary cellular line MG9, MG11 and MG12 and (g – h). TEER max and sodium fluorescein transport min data of MG9, MG11 and MG12. Data were rep-resented as mean ± SD (n = 3) and * above indicate the differences between the three cell lines at $p < 0.05$.

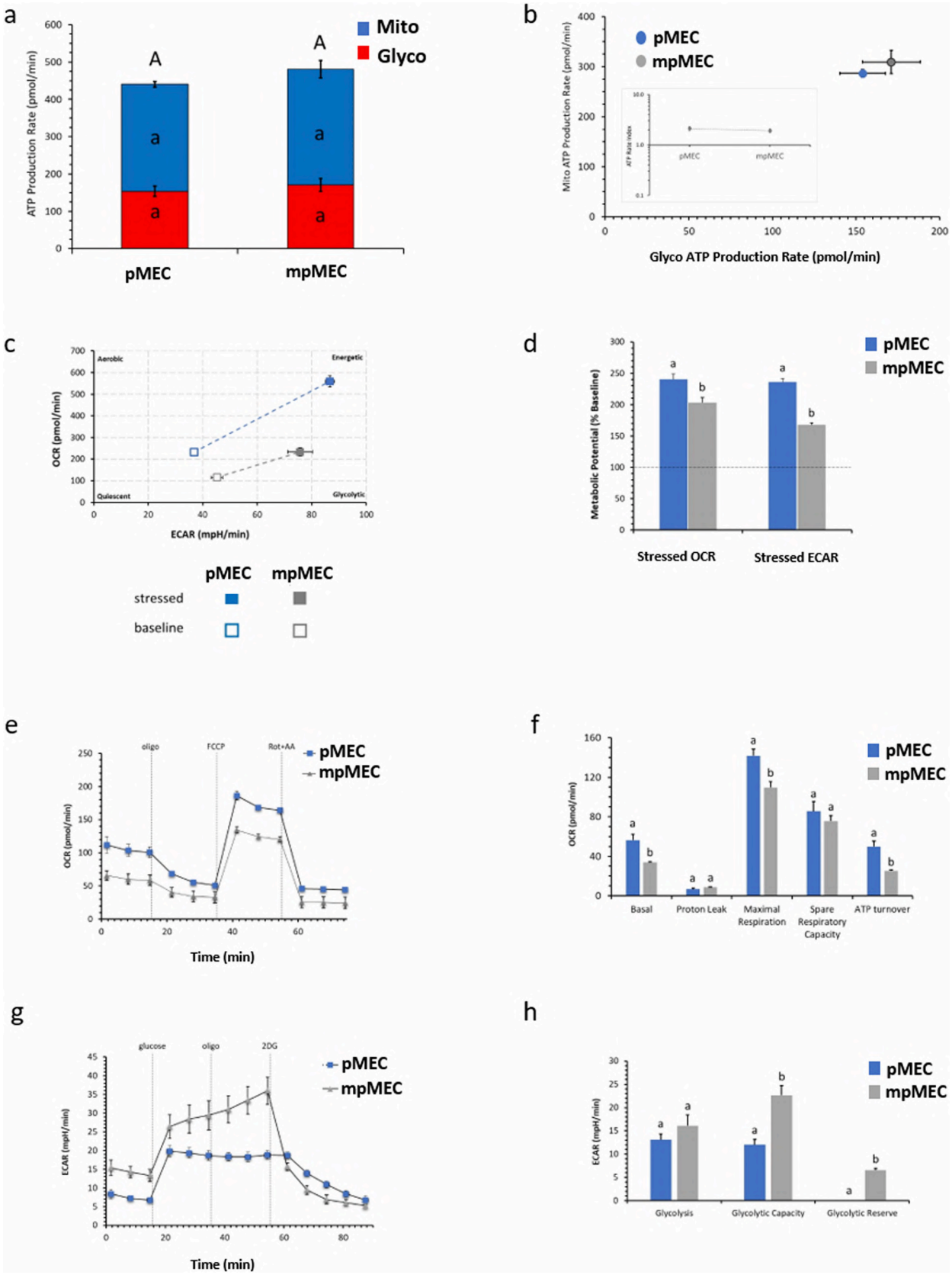

(caption on next page)

Fig. 5. Bioenergetic metabolism in mpMECs *vs* pMECs. a) Evaluation of the real-time ATP production rate by mitochondrial OXPHOS (■, blue) or by glycolysis (■, red). Different lower-case letters indicate significantly different values ($p \leq 0.05$) among cell lines in the same metabolic pathway; different upper-case letters indicate different values ($p \leq 0.05$) among cell lines in ATP production rates due to the sum of OXPHOS plus glycolysis. b) Energy map with Mito- *vs* Glyco-ATP production of pMECs (●, blue spheres) and mpMECs (●, grey spheres) are plotted. The insert plot shows the ratio between the mitochondrial ATP production rate and the glycolytic ATP production rate (logarithmic scale). c) Phenogram illustrates the relative metabolic state of MEC cells of baseline (empty squares) and stressed (full squares) phenotypes of pMECs (blue squares) and mpMECs (grey squares). d) Metabolic potential in "Stressed OCR" or "Stressed ECAR" is expressed as % "Baseline OCR" and "Baseline ECAR" (dashed horizontal line), in pMECs or mpMECs. Different letters indicate significant differences ($p \leq 0.05$) among treatments within the same parameter. e) Oxygen consumption rate (OCR) profile under basal respiration conditions and after the addition of 1.5 μM oligomycin (olig), 1.0 μM FCCP and a mixture of 0.5 μM rotenone plus antimycin A (rot+AA) in pMECs or mpMECs. Compound injections are shown as dotted lines. f) Mitochondrial parameters: basal respiration, proton leak, maximal respiration, spare respiratory capacity, ATP turnover. Different letters indicate significant differences ($p \leq 0.05$) among treatments within the same parameter. g) Extracellular acidification rate (ECAR) profile under basal conditions and after the addition of 10 mM glucose, 5 μM oligomycin (olig), and 50 mM 2-deoxyglucose (2-DG). Injections are shown as dotted lines. (H) Parameters of the glycolytic function: glycolysis, glycolytic capacity, and glycolytic reserve. Different letters indicate significant differences ($p \leq 0.05$) among treatments within the same parameter. Data expressed as column charts (a, d, f, h) or points (b, c, e, g) represent the mean ± SD (vertical bars). (For interpretation of the references to colour in this figure legend, the reader is referred to the web version of this article.)

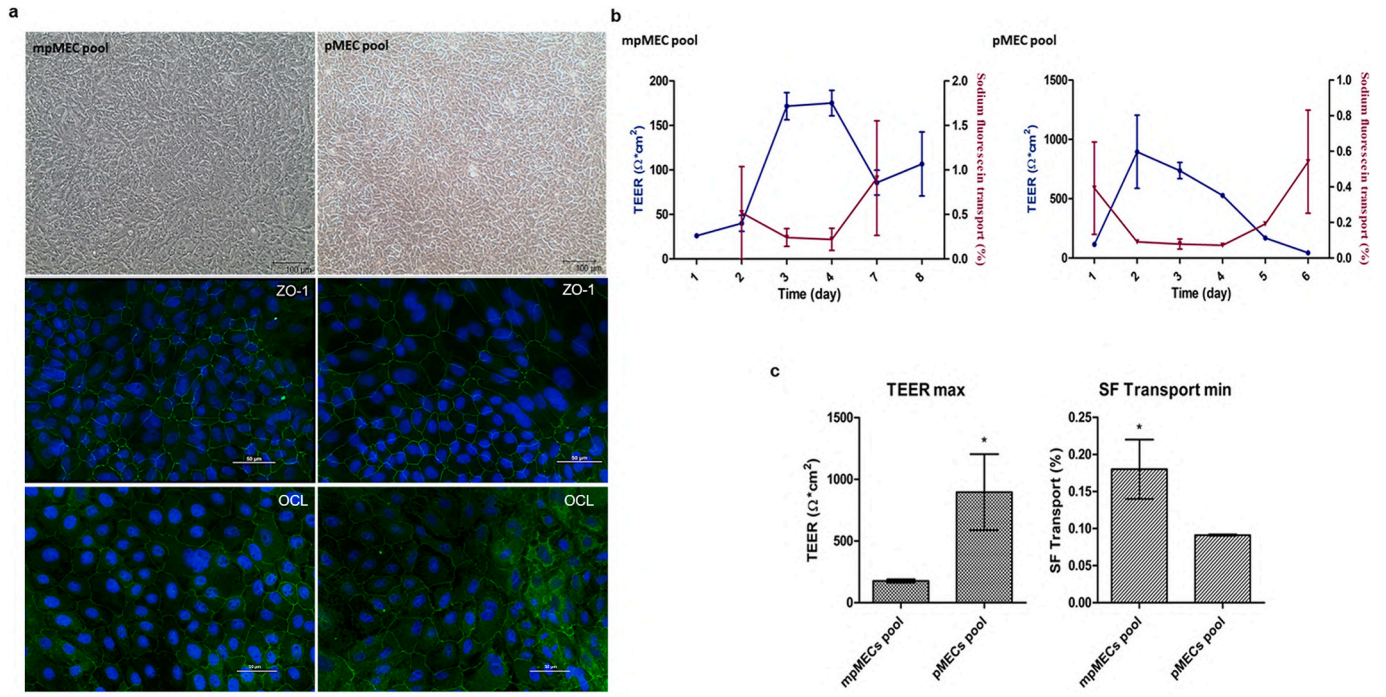

Fig. 6. mpMEC *vs* pMECs barrier a) mpMECs and pMECs grow compact on transwell and expressed tight junctions: ZO-1 and OCL. b) mpMEC pool TEER (Ω*cm^2), graphs on the left and, SF transport (%), graphs on the right, c) pMEC pool TEER (Ω*cm^2), graphs on the left and, SF transport (%), graphs on the right d) TEER value max and minimum SF transport value in mpMEC pool and pMEC pool. Data were represented as mean ± SD (n = 3) and * above indicate the significative differences at $p < 0.05$.

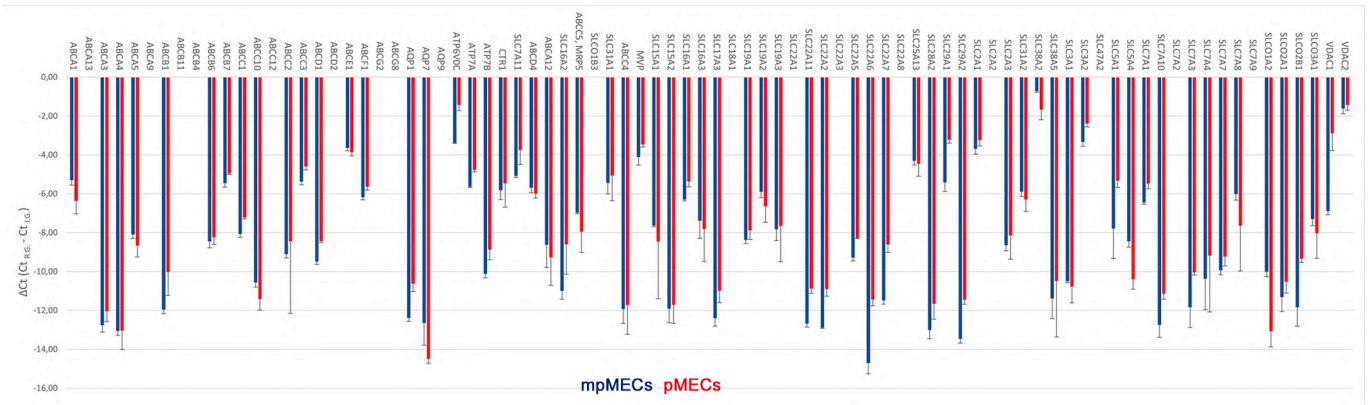

Fig. 7. Transcriptional profile for Pig Drug Transporter mpMECs (blue bar charts) and pMECs (red bar charts). The eighty-four genes analysed were represented as relative expression calculated as ΔCt (mean Ct reference genes – Ct interest genes) ± SD (n = 3). (For interpretation of the references to colour in this figure legend, the reader is referred to the web version of this article.)

there are very few studies on *in vitro* permeability models to estimate drug transport across mammary epithelium, from all these studies resulted evident that a tight monolayer is required to evaluate transport across biological barrier including the mammary one (Nauwelaerts et al., 2021).

In our previous study we described for the first time the ability to porcine epithelial cells to create a tight monolayer (Bernardini et al., 2021b), in the present research, although with different quantitative and kinetic patterns, the three minipig cell lines were able to create a tight monolayer by expressing the two tight junctions proteins ZO-1 and OCL, both of which are essentials for epithelial junctions and thus for epithelial barrier formation. Measurement of TEER and SF transport indicated that all the three mpMEC primary lines obtained are able to create the epithelial barrier under standardized culture conditions that allow transport experiments to be performed for at least two consecutive days.

Since Göttingen Minipigs use in biomedical research is increasing due to their smaller size, genetic and microbiological stability and temperament that makes them easier to manage in a lab setting, especially in pharmaceutical research, the ConcePTION Consortium chose this breed and we decided to carry out a comparative study of mpMECs *versus* pMECs to evidence possible differences on cellular features. Considering that morphological characterization and expression of epithelial markers didn't evidence any differences between mpMECs and pMECs, we studied if differences in bioenergetic profiles exist. Although total and aerobic or anaerobic ATP productions were not different, pMECs made more efficient use of mitochondrial oxidative metabolism than mpMECs. Conversely, mpMECs could more efficiently increase the glycolytic activity than pMEC. This different cellular metabolic behaviour is consistent (Vander Heiden et al., 2009; Wang et al., 2022) with the different proliferation rate, in fact comparing doubling time, mpMECs are more proliferative than pMECs (30,19 ± 3,80 *vs* 46,20 ± 2,71).

Comparing the mpMEC and pMEC ability to create the epithelial barrier, the main difference is in the absolute TEER values reached, with commercial hybrid pig cells TEER value higher than those of minipigs and this difference is very clearly reflected in SF transport results. The TEER values obtained from mpMECs seem more similar to those obtained by Kimura et al. (Kimura et al., 2006) in human using mammary primary cell cultures not immortalized. Overall, it's possible affirm that mpMECs possess the ability to create the epithelial barrier even if less tight than MECs isolated from hybrid pig. Anyway, our results seem to indicate that epithelial barrier created by mpMECs is more similar to that obtained with human mammary epithelial cells, this could suggest that mpMECs could be the best candidates for translational purposes.

The changes of the drug transporter gene expression among the physiological stages of the mammary gland are very impressive (García-Lino et al., 2019). In this regard, we have deepened our study by analysing the drug transporters gene expression profile of mpMECs compared with pMECs. Our results indicated that both expressed 66 out of the 84 analysed genes, including genes belonging to ATP-binding cassette (ABC-) and Solute Carrier (SLC-) transporters. Some of the not expressed genes, like as SLC22A1 and ABCG2, increased their expression during lactation in mammary gland (García-Lino et al., 2019; Ventrella et al., 2019), so our results are consisting with the fact that cells were isolated from resting mammary gland. Overall, our results indicated very limited differences in drug transporter gene expression between mpMECs and pMECs.

5. Conclusion

This is the first report on the establishment of primary mammary epithelial cell lines from Göttingen Minipigs. Differences among primary cells obtained from animals of different breeds, sexes and ages may lead to reduced reproducibility of experimental data, in particular when used for translational purposes. Studies on the passage of drugs across the blood/milk barrier are necessary to define a safer environment for breastfeeding and the main value of the porcine model is the possibility of *in vivo* screening for oral/IM/IV dosing by comparison with human data. The IVIVC approach has great potential, but standardization of the models used is essential. By comparing mpMECs with mammary epithelial cell lines isolated from hybrid pigs we concluded that, although both cell lines showed the ability to create an epithelial barrier, some differences that exist. These line-dependent differences should always be considered when the Göttingen Minipigs is used as a large animal model for translational studies involving IVIVC. Overall, the results obtained in this paper lay solid foundations for building more complex cellular models *in vitro*, in which, for example, the vascular component could be introduced to mimic the alveolar architecture.

Funding

The ConcePTION project has received funding from the Innovative Medicines Initiative 2 Joint Undertaking under grant agreement No. 821520. This Joint Undertaking receives support from the European Union's Horizon 2020 research and innovation program and EFPIA.

Contributions

Conceptualization and design of the experiments C.B. and M.F. Execution of experiments and acquisition of data: C.B., S.N., D.L.M., R. S., N.N., D.V., A.E. and F.T. Data analysis and interpretation: C.B., S.N., A.Z. and M.F. Writing of original draft: C.B., S.N., D.L.M. and M.F. All authors reviewed, edited and approved the final manuscript.

Ethics declarations

All samples were collected with approval of the Animal Care Committee, Italian Ministry of Health as dictated by D.Lgs 26/2014 (approval n° 32/2021-PR).

CRediT authorship contribution statement

Chiara Bernardini: Writing – review & editing, Writing – original draft, Visualization, Methodology, Formal analysis, Data curation, Conceptualization. **Salvatore Nesci:** Writing – original draft, Visualization, Methodology, Formal analysis, Data curation. **Debora La Mantia:** Writing – review & editing, Writing – original draft, Methodology, Formal analysis, Data curation. **Roberta Salaroli:** Methodology, Formal analysis, Data curation. **Nina Nauwelaerts:** Methodology, Formal analysis, Data curation. **Domenico Ventrella:** Visualization, Methodology, Investigation. **Alberto Elmi:** Methodology, Investigation. **Fabiana Trombetti:** Supervision, Investigation. **Augusta Zannoni:** Methodology, Formal analysis, Data curation. **Monica Forni:** Visualization, Supervision, Funding acquisition, Conceptualization.

Declaration of competing interest

The authors declare no conflict of interest.

Availability of data and materials

Data are available on AMSActa Institutional Research Repository by AlmaDL University of Bologna Digital Library: https://doi.org/10.6092/unibo/amsacta/7210.

Acknowledgements

NN acknoweledges her PhD scholarship (Research-Foundation-Flanders 1S50721N).

References

Adam, M.P., Polifka, J.E., Friedman, J.M., 2011. Evolving knowledge of the teratogenicity of medications in human pregnancy. Am. J. Med. Genet. C: Semin. Med. Genet. 157C, 175–182. https://doi.org/10.1002/ajmg.c.30313.

Algieri, C., Bernardini, C., Trombetti, F., Schena, E., Zannoni, A., Forni, M., Nesci, S., 2022. Cellular metabolism and bioenergetic function in human fibroblasts and preadipocytes of type 2 familial partial lipodystrophy. Int. J. Mol. Sci. 23, 8659. https://doi.org/10.3390/ijms23158659.

Ashkenazi, N., Ventrella, D., 2020. Report on Lactation Characteristics of Animal Species; Selection of the Animal Species to be Used in in Vivo Studies (D3.2). https://doi.org/10.5281/zenodo.5825282.

Bernardini, C., Nauwelaerts, N., 2021. Report on Characterization in Vitro Human/Animal Mammary Epithelial Cell Cultures Models, Including Comparison between in Vitro Models (D3.3). https://doi.org/10.5281/zenodo.5825334.

Bernardini, C., Algieri, C., Mantia, L.D., Zannoni, A., Salaroli, R., Trombetti, F., Forni, M., Pagliarani, A., Nesci, S., 2021a. Relationship between serum concentration, functional parameters and cell bioenergetics in IPEC-J2 cell line. Histochem. Cell Biol. https://doi.org/10.1007/s00418-021-01981-2.

Bernardini, C., La Mantia, D., Salaroli, R., Zannoni, A., Nauwelaerts, N., Deferm, N., Ventrella, D., Bacci, M.L., Sarli, G., Bouisset-Leonard, M., Annaert, P., Forni, M., 2021b. Development of a pig mammary epithelial cell culture model as a non-clinical tool for studying epithelial barrier—a contribution from the IMI-ConcePTION project. Animals 11, 2012. https://doi.org/10.3390/ani11072012.

Bernardini, C., La Mantia, D., Salaroli, R., Ventrella, D., Elmi, A., Zannoni, A., Forni, M., 2023. Isolation of vascular wall mesenchymal stem cells from the thoracic aorta of adult Göttingen Minipigs: a new protocol for the simultaneous endothelial cell collection. Animals 13, 2601. https://doi.org/10.3390/ani13162601.

Bin, C., Ning, W., 2016. Large animal stroke models vs. rodent stroke models, pros and cons, and combination? Acta Neurochir. (Supplement 121) https://doi.org/10.1007/978-3-319-18497-5_13.

Bollen, P., Ellegaard, L., 1997. The Göttingen minipig in pharmacology and toxicology. Pharmacol. Toxicol. 80 (Suppl. 2), 3–4. https://doi.org/10.1111/j.1600-0773.1997.tb01980.x.

ConcePTION [WWW Document], n.d. URL https://www.imi-conception.eu/ (accessed 3.6.23).

Dahanayaka, S., Rezaei, R., Porter, W.W., Johnson, G.A., Burghardt, R.C., Bazer, F.W., Hou, Y.Q., Wu, Z.L., Wu, G., 2015. Technical note: isolation and characterization of porcine mammary epithelial cells1,2. J. Anim. Sci. 93, 5186–5193. https://doi.org/10.2527/jas.2015-9250.

Festing, M.F.W., 2004. Refinement and reduction through the control of variation. Altern. Lab. Anim 32 (Suppl 1A), 259–263. https://doi.org/10.1177/026119290403201s43.

Flisikowska, T., Egli, J., Flisikowski, K., Stumbaum, M., Küng, E., Ebeling, M., Schmucki, R., Georges, G., Singer, T., Kurome, M., Kessler, B., Zakhartchenko, V., Wolf, E., Weber, F., Schnieke, A., Iglesias, A., 2022. A humanized minipig model for the toxicological testing of therapeutic recombinant antibodies. Nat. Biomed. Eng. 6, 1248–1256. https://doi.org/10.1038/s41551-022-00921-2.

Forster, R., Ancian, P., Fredholm, M., Simianer, H., Whitelaw, B., Steering Group of the RETHINK Project, 2010. The minipig as a platform for new technologies in toxicology. J. Pharmacol. Toxicol. Methods 62, 227–235. https://doi.org/10.1016/j.vascn.2010.05.007.

García-Lino, A.M., Álvarez-Fernández, I., Blanco-Paniagua, E., Merino, G., Álvarez, A.I., 2019. Transporters in the mammary gland-contribution to presence of nutrients and drugs into milk. Nutrients 11. https://doi.org/10.3390/nu11102372.

Gohar, F., Gohar, A., Hülskamp, G., Debus, O., 2018. The translational medicine professional: a bridge between bench and bedside? Front. Med. 5 https://doi.org/10.3389/fmed.2018.00294.

Karlsson, M., Sjöstedt, E., Oksvold, P., Sivertsson, Å., Huang, J., Álvez, M.B., Arif, M., Li, X., Lin, L., Yu, J., Ma, T., Xu, F., Han, P., Jiang, H., Mardinoglu, A., Zhang, C., von Feilitzen, K., Xu, X., Wang, J., Yang, H., Bolund, L., Zhong, W., Fagerberg, L., Lindskog, C., Pontén, F., Mulder, J., Luo, Y., Uhlen, M., 2022. Genome-wide annotation of protein-coding genes in pig. BMC Biol. 20, 25. https://doi.org/10.1186/s12915-022-01229-y.

Kimura, S., Morimoto, K., Okamoto, H., Ueda, H., Kobayashi, D., Kobayashi, J., Morimoto, Y., 2006. Development of a human mammary epithelial cell culture model for evaluation of drug transfer into milk. Arch. Pharm. Res. 29, 424–429. https://doi.org/10.1007/BF02968594.

Kobayashi, E., Hanazono, Y., Kunita, S., 2018. Swine used in the medical university: overview of 20 years of experience. Exp. Anim. 67, 7–13. https://doi.org/10.1538/expanim.17-0086.

La Mantia, D., Bernardini, C., Zannoni, A., Salaroli, R., Wang, C., Bencivenni, S., Forni, M., 2022. Efficacy of stem cell therapy in large animal models of ischemic cardiomyopathies: a systematic review and meta-analysis. Animals 12, 749. https://doi.org/10.3390/ani12060749.

Leenaars, C.H.C., Kouwenaar, C., Stafleu, F.R., Bleich, A., Ritskes-Hoitinga, M., De Vries, R.B.M., Meijboom, F.L.B., 2019. Animal to human translation: a systematic scoping review of reported concordance rates. J. Transl. Med. 17, 223. https://doi.org/10.1186/s12967-019-1976-2.

Levi, M., Salaroli, R., Parenti, F., De Maria, R., Zannoni, A., Bernardini, C., Gola, C., Brocco, A., Marangio, A., Benazzi, C., Muscatello, L.V., Brunetti, B., Forni, M., Sarli, G., 2021. Doxorubicin treatment modulates chemoresistance and affects the cell cycle in two canine mammary tumour cell lines. BMC Vet. Res. 17, 30. https://doi.org/10.1186/s12917-020-02709-5.

Li, S., Fisher, M., 2023. Improving large animal ischemic stroke models for translational studies in the era of recanalization. Stroke 54, e16–e19. https://doi.org/10.1161/STROKEAHA.122.041354.

Müller, C., Marzahn, U., Kohl, B., Sayed, K.E., Lohan, A., Meier, C., Ertel, W., Schulze-Tanzil, G., 2013. Hybrid pig versus Göttingen minipig-derived cartilage and chondrocytes show pig line-dependent differences. Exp. Biol. Med. (Maywood) 238, 1210–1222. https://doi.org/10.1177/1535370213502630.

Nauwelaerts, N., Deferm, N., Smits, A., Bernardini, C., Lammens, B., Gandia, P., Panchaud, A., Nordeng, H., Bacci, M.L., Forni, M., Ventrella, D., Van Calsteren, K., DeLise, A., Huys, I., Bouisset-Leonard, M., Allegaert, K., Annaert, P., 2021. A comprehensive review on non-clinical methods to study transfer of medication into breast milk – a contribution from the ConcePTION project. Biomed. Pharmacother. 136, 111038 https://doi.org/10.1016/j.biopha.2020.111038.

Nörby, U., Noël-Cuppers, B., Hristoskova, S., Desai, M., Härmark, L., Steel, M., El-Haddad, C., Douarin, L., 2021. Online information discrepancies regarding safety of medicine use during pregnancy and lactation: an IMI ConcePTION study. Expert Opin. Drug Saf. 20, 1117–1124. https://doi.org/10.1080/14740338.2021.1935865.

Pabst, R., 2020. The pig as a model for immunology research. Cell Tissue Res. 380, 287–304. https://doi.org/10.1007/s00441-020-03206-9.

Robinson, N.B., Krieger, Katherine, Khan, F.M., Huffman, W., Chang, M., Naik, A., Yongle, R., Hameed, I., Krieger, Karl, Girardi, L.N., Gaudino, M., 2019. The current state of animal models in research: a review. Int. J. Surg. 72, 9–13. https://doi.org/10.1016/j.ijsu.2019.10.015.

Rojas, A., Gonzalez, I., Figueroa, H., 2008. Cell line cross-contamination in biomedical research: a call to prevent unawareness. Acta Pharmacol. Sin. 29, 877–880. https://doi.org/10.1111/j.1745-7254.2008.00809.x.

Sazzad, F., Kollengode, R., Beverly, C.L.X., Kiat, T.Y., Ganesh, G., Kofidis, T., 2023. Preclinical large animal in-vivo experiments for surgically implanted atrioventricular valve: reappraisal and systematic review. Curr. Cardiol. Rev. 19, e170622206130 https://doi.org/10.2174/1573403X18666220617115216.

Simianer, H., Köhn, F., 2010. Genetic management of the Göttingen Minipig population. J. Pharmacol. Toxicol. Methods 62, 221–226. https://doi.org/10.1016/j.vascn.2010.05.004.

Singh, V.K., Thrall, K.D., Hauer-Jensen, M., 2016. Minipigs as models in drug discovery. Expert Opin. Drug Discovery 11, 1131–1134.

Sturek, M., Alloosh, M., Sellke, F.W., 2020. Swine disease models for optimal vascular engineering. Annu. Rev. Biomed. Eng. 22, 25–49. https://doi.org/10.1146/annurev-bioeng-082919-053009.

Tang, H., Mayersohn, M., 2018. Porcine prediction of pharmacokinetic parameters in people: a pig in a poke? Drug Metab. Dispos. 46, 1712–1724. https://doi.org/10.1124/dmd.118.083311.

Tubon, I., Zannoni, A., Bernardini, C., Salaroli, R., Bertocchi, M., Mandrioli, R., Vinueza, D., Antognoni, F., Forni, M., 2019. In vitro anti-inflammatory effect of *Salvia sagittata* ethanolic extract on primary cultures of porcine aortic endothelial cells. Oxidative Med. Cell. Longev. 2019, 1–11. https://doi.org/10.1155/2019/6829173.

van der Graaf, R., van der Zande, I.S.E., van Delden, J.J.M., 2019. How the CIOMS guidelines contribute to fair inclusion of pregnant women in research. Bioethics 33, 367–373. https://doi.org/10.1111/bioe.12520.

van der Laan, J.W., Brightwell, J., McAnulty, P., Ratky, J., Stark, C., Steering Group of the RETHINK Project, 2010. Regulatory acceptability of the minipig in the development of pharmaceuticals, chemicals and other products. J. Pharmacol. Toxicol. Methods 62, 184–195. https://doi.org/10.1016/j.vascn.2010.05.005.

Vander Heiden, M.G., Cantley, L.C., Thompson, C.B., 2009. Understanding the Warburg effect: the metabolic requirements of cell proliferation. Science 324, 1029–1033. https://doi.org/10.1126/science.1160809.

Ventrella, D., Forni, M., Bacci, M.L., Annaert, P., 2019. Non-clinical models to determine drug passage into human breast milk. CPD 25, 534–548. https://doi.org/10.2174/1381612825666190320165904.

Ventrella, D., Ashkenazi, N., Elmi, A., Allegaert, K., Aniballi, C., DeLise, A., Devine, P.J., Smits, A., Steiner, L., Forni, M., Bouisset-Leonard, M., Bacci, M.L., 2021. Animal models for in vivo lactation studies: anatomy, physiology and milk compositions in the most used non-clinical species: a contribution from the ConcePTION project. Animals 11, 714. https://doi.org/10.3390/ani11030714.

Wang, Y., Stancliffe, E., Fowle-Grider, R., Wang, R., Wang, C., Schwaiger-Haber, M., Shriver, L.P., Patti, G.J., 2022. Saturation of the mitochondrial NADH shuttles drives aerobic glycolysis in proliferating cells. Mol. Cell 82, 3270–3283.e9. https://doi.org/10.1016/j.molcel.2022.07.007.

Weber-Levine, C., Hersh, A.M., Jiang, K., Routkevitch, D., Tsehay, Y., Perdomo-Pantoja, A., Judy, B.F., Kerensky, M., Liu, A., Adams, M., Izzi, J., Doloff, J.C., Manbachi, A., Theodore, N., 2022. Porcine model of spinal cord injury: a systematic review. Neurotrauma Rep. 3, 352–368. https://doi.org/10.1089/neur.2022.0038.

Zaniboni, A., Bernardini, C., Alessandri, M., Mangano, C., Zannoni, A., Bianchi, F., Sarli, G., Calzà, L., Bacci, M.L., Forni, M., 2014. Cells derived from porcine aorta tunica media show mesenchymal stromal-like cell properties in in vitro culture. Am. J. Phys. Cell Phys. 306, C322–C333. https://doi.org/10.1152/ajpcell.00112.2013.